Photovoltaic Enhanced UHF RFID Tag Antennas for Dual Purpose Energy Harvesting

Alanson P. Sample, Jeff Braun, Aaron Parks, and Joshua R. Smith
Department of Electrical Engineering
University of Washington
Seattle Washington, USA
{alanson, jbraun, anparks}@u.washington.edu, jrs@cs.washington.edu

***Abstract*—The most significant barrier to improving passive RFID tag performance for both fixed function ID tags and enhanced RFID tags is the limitation on the amount of power that can be harvested for operation. This paper presents a novel approach for incorporating solar harvesting capability into existing passive RFID tags without increasing the parts count or changing the tag assembly process. Our approach employs the tag's antenna as a dual function element in which the antenna simultaneously harvests RF energy, communicates with the RFID reader, and harvests solar energy for auxiliary power. This is accomplished by using low cost, printable photovoltaics deposited on flexible substrate to form part of the antenna's radiating structure. Several prototype UHF RFID antennas are demonstrated using commercially available thin film, amorphous solar cells. To quantify the improvement in tag performance, Intel's WISP was used as an initial test vehicle. The effective read range of the tag was increased by six times and exceeded the reader's sensitivity limitations. Additionally, the new antenna allowed for sensing and computing operations to take place independent of the RFID reader under typical office lighting conditions.**

Keywords - Passive RFID; Solar; Antenna; Energy Harvesting

I. INTRODUCTION

Development in Radio Frequency Identification (RFID) technology has produced battery-free RFID tags, capable of wirelessly reporting a unique ID over a distance of several meters while exclusively powered by harvested RF energy. Although the functionality of these commercial RFID tags is extremely limited, today's tags are essentially a wireless micro-computing platform, with an RF transceiver and a nearly unlimited lifetime. Several research efforts are pushing passive RFID beyond simple barcode replacement and are exploring the broader space of wirelessly powered devices. These enhanced RFID tags transcend the rigid EPC classification structure, providing sensing, arbitrary computing, data logging, user interfacing, and actuation functionality, all while powered wirelessly by the RFID reader [1-6]. As future applications demand greater RFID tag functionality and increased operating range, the amount of harvestable power will become an even more critical design constraint.

The reliance of RFID tags on power transmitted from RFID readers creates two significant limitations. First, the operational region of a tag is limited to the physical zone covered by the RFID reader. Tags outside the zone are left un-powered. This means that, in order to increase the space over which the tag can operate, it is necessary to increase the number of RFID readers and reader antennas to cover the larger space. This can be cost prohibitive and requires significant effort to effectively instrument an environment. Thus, most RFID applications are limited to a specific, well defined work space, or the RFID tags are only read (i.e. powered on) at gateways or portals for tracking purposes. Important applications like logging of sensor data during shipping do not appear to be practical using only reader power, as the infrastructure necessary to instrument such a large area with readers would be prohibitively expensive.

The second limitation resulting from reliance on reader power is that, from the tag's perspective, available power varies unpredictably as the tag is moved throughout the reader's coverage zone. This is particularly limiting for enhanced RFID tags, where different tasks such as sensing, computing, storing data, and communication require different amounts of power. Therefore, it is desirable to utilize additional energy sources to increase the functionality, read range, reliability, and read rate of RFID tags.

There are a variety of energy sources that may be harnessed to power enhanced RFID tags, such as solar, thermal, mechanical vibration, or ambient RF energy. Harvestable energy from these sources varies from less than one μW to a few mW, depending on the technology and environment [7]. Initial work combining solar cells with RFID tags has shown promising results [8,9]. However, these techniques are not compatible with traditional high volume RFID manufacturing techniques. Both solutions require a bulky and costly external crystal silicon solar cell, approximately the size of a small battery pack. Considering that the small size and low cost of RFID tags are the key features that enable their ubiquitous deployment; it is necessary that the enhancement of a tag with a photovoltaic power source not reduce the deployability of the device.

This paper presents a novel, dual purpose RFID tag antenna that simultaneously harvests RF energy, communicates with the RFID reader, and harvests solar energy for auxiliary power. The goal is to leverage modern printed photovoltaic manufacturing techniques, which produce thin, low-cost, flexible solar cells, and integrate them into printed RFID

antennas. This work presents an initial prototype, which shows the feasibility of construction of a solar-enhanced antenna for an RFID IC. Additionally a WISP tag is augmented with a solar-enhanced antenna, yielding a 6x range improvement. Finally, reader-independent operation is explored using a solar-enhanced WISP under typical office lighting conditions.

II. System Overview

In order for a solar-enhanced RFID antenna to be successfully integrated into either fixed function ID or enhanced RFID tags, it is necessary that the replacement of the standard antenna with solar cells does not alter the manufacturability or usability of the device. Recent breakthroughs in printed electronics have allowed for low cost, printed solar cells that can be manufactured in high volume and in a roll-to-roll process [10]. Generally speaking, the manufacturing processes for solar cells are compatible with present day RFID antenna printing techniques, although there can be variations between manufacturers due to the type of application and the material properties. In both cases, metal traces for DC electrodes and antenna elements can be screen printed, applied with a material printer, or chemically deposited and etched. Solar material is typically applied as a thin film with a squeegee type application, screen printing process, or deposited with a material printer [10].

There are several examples of solar cells integrated with antennas. The authors in [11] present a GPS patch antenna that employs a poly crystalline solar cell patterned on the patch element. Additionally, solar-enhanced slot antennas are presented in [12-14], which utilize amorphous silicon cells on a flexible substrate. These efforts focus on the advantages of a fully integrated design, which reduces size and weight, while maximizing surface area for solar harvesting. However, the amount of power gained by reusing the relatively small surface area of the antenna for power harvesting does not significantly improve the power budgets for the proposed applications, which include satellites, GPS for motor vehicles, and battery powered consumer electronics.

The opposite is true for RFID tags, where the power that can be harvested by photovoltaics covering the RFID label's surface area is sufficient to completely power the tag. As an example, PowerFilm, Inc. manufactures flexible, thin-film solar cells that produce 2-4 mW/cm^2 under full sunlight. This means that even under low lighting conditions, where only a fraction of this power is available, there will be ample power for RFID ICs. Typically RFID tags consume between 10uW to 100uW of power.

Figure 1 shows a conceptual diagram of a solar-enhanced RFID tag. The antenna can be printed on to standard, flexible substrates, with the antenna electrodes themselves printed in copper or silver. The key attribute of this design is that the solar cell is part of the radiating structure of the antenna. This has the advantage of keeping the overall surface area of the final label consistent with current standard label designs as well as reducing material costs. In order to optimize the benefits of the solar antenna, the solar panel's area and number of cells must be selected based on the requirements of the application and the particular RFID IC used.

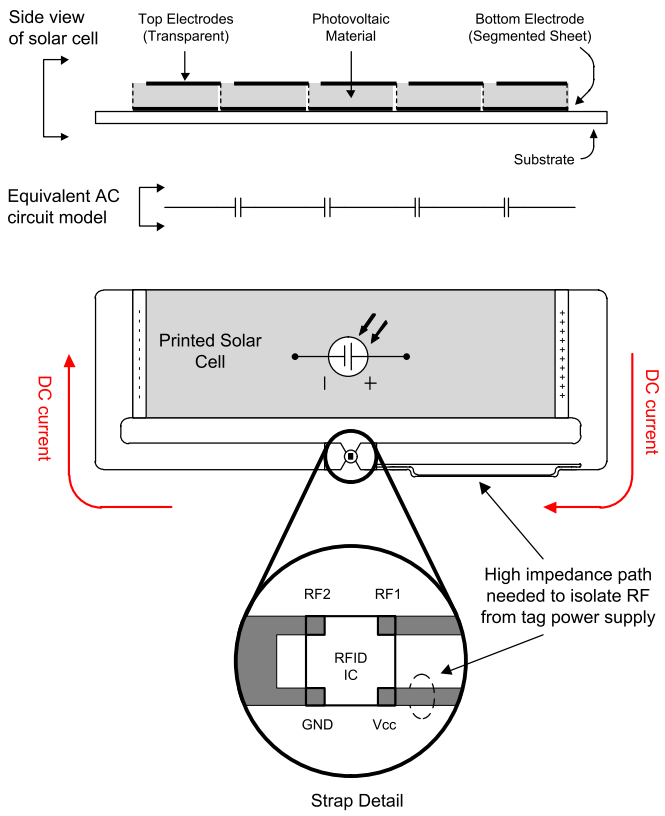

Figure 1. Conceptual diagram of a solar-enhanced RFID tag antenna with RFID IC. VCC is connected to the positive bus of the solar cell via a high-impedance trace. RF2 and Ground are connected to the same port of the antenna, and RF1 is connected opposite them.

The top image in Figure 1 shows an exaggerated side view of a typical amorphous silicon solar cell unit. Since the individual cells are connected in series to produce the desired output voltage, the positive and negative electrodes of each cell are interleaved, creating a highly capacitive interface. One might assume that the PN junction of the solar cell would rectify the RF signal. However, at UHF frequencies, the RF energy takes the low impedance "capacitive" path between electrodes. The result is the AC equivalent model shown below the side view in Figure 1. Since the capacitance of the junctions is effectively very large, the cell performs very similarly to a uniform metal sheet at UHF frequencies.

In order to use the solar energy harvested by the hybrid antenna, the RFID tag must be able to accept DC power as well as RF signals. To achieve this, the IC will need to be modified to expose the un-regulated power supply node, which is typically the rectifier output. Considering that many commercial RFID tags are four pin devices providing two ground connections, it is reasonable to repurpose one of the redundant ground pins for DC input. This is highlighted in the 'strap detail' in Figure 1. The last major design challenge is to ensure proper isolation between the DC power input and the RF signal so that RF noise does not compromise the performance of the IC. We propose using a thin metal trace that presents a high impedance path to the RF signal while allowing DC power to pass through to the IC.

III. Two Solar-Enhanced RFID Antenna Designs

The following sections describe the design and performance of two distinct solar-enhanced antennas. The first antenna presented is designed specifically for an RFID IC, and is intended to show the viability of constructing a low cost, size reduced antenna with integrated solar cells. Unfortunately, to date, there are no commercially available RFID ICs that expose the internal, unregulated power supply node. Thus, this first photovoltaic-enhanced antenna will only be able to demonstrate the RF antenna performance and not the impact that increased power will have on tag performance.

The second antenna design presented aims to show the benefit of increased available power provided by a photovoltaic-enhanced tag antenna on system performance using Intel Lab's open-source WISP 4.1 platform [4]. The WISP is a fully passive (battery free) PCB RFID tag, and has the unregulated power supply pin exposed so that the tag's power source may be augmented. Although the WISP has many similar attributes to conventional RFID devices, it is not a direct stand-in for a commercial IC tag. Notably, the read range is less than half that of a commercial RFID tag, and the input impedance of the WISP is very different than an IC tag and thus requires a different antenna design.

It is hoped that by validating the RF performance of the IC-specific solar antenna design, and by presenting the performance benefits of a solar antenna with the WISP, that the viability of a complete system consisting of a photovoltaic enhanced antenna plus a custom RFID IC with exposed unregulated power pin can be concluded.

A. Protoype Solar Antenna Design for RFID ICs

Figure 2 illustrates the proposed IC-specific solar antenna design. The operation of the antenna can be viewed as a monopole mirrored over the solar cell, which is acting as a ground plane. An inductive strap is added to provide the necessary reactance to conjugate match to the capacitive RFID IC. The vertical section of the antenna arm (shown with length 8.2mm) can be varied to tune the resonant frequency of the antenna. The small spiral on the end of the antenna enables additional fine tuning of reactance.

In order to draw power from the solar cell, the DC bus bars located at the two ends of the cell need to be connected to the IC. To accomplish this, the antenna's arm was relocated to the top of the cell and connected to the negative terminal of the solar cell. This allows the inductive strap and the GND pin of the tag to be at the same DC voltage potential. The positive terminal of the solar cell is located at the bottom and a thin trace is added to connect it to the IC. This can be seen in the detail pop out in Figure 2, where an RFID IC with an extra terminal is shown connected to the antenna.

Figure 3 shows an image of the constructed photovoltaic-enhanced RFID antenna. The metal traces were cut with an automatic stencil cutter and mounted to a 1 mm thick Plexiglas backing for rigidity and testing purposes. The solar cell used in this prototype is the Powerfilm SP3-37 amorphous silicon solar cell. This particular solar cell is chosen because of its relatively small size, flexibility, and because it is produced through a low-cost roll-to-roll printing process. This low-cost manufacturing means that, in the future, the overall cost of large-scale production for the solar-enhanced antenna will be inexpensive and compatible with current RFID tag manufacturing processes. The prototype antenna is built on Plexiglas substrate for the purposes of this experiment, but in a real world application would likely be printed, along with the solar cell, onto a flexible substrate similar to current RFID tags. The SP3-37 solar cell has an peak output of 3.0v at 22mA under full sunlight (107,527 Lux) and an output of 2.5v at 100uA under typical office lighting (330 Lux).

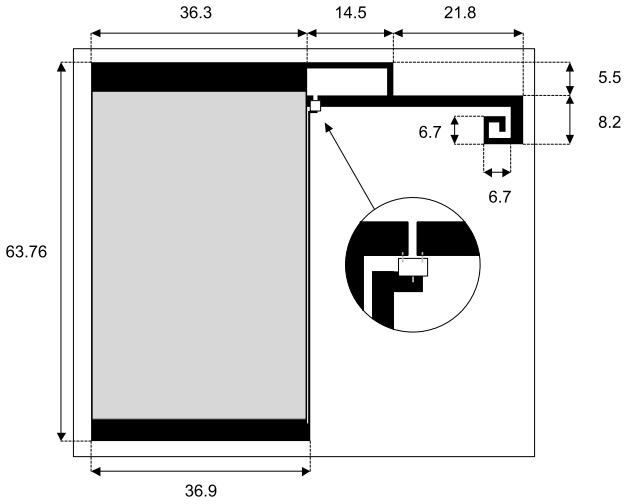

Figure 2. Diagram of the photovoltaic-enhanced antenna for an RFID IC. Solid black lines denote copper traces. The gray section represents the solar cell. A small, thin trace connects the positive terminal (bottom) of the solar cell to the IC, providing DC power. Lengths are given in mm, and trace widths are 1mm and 2mm.

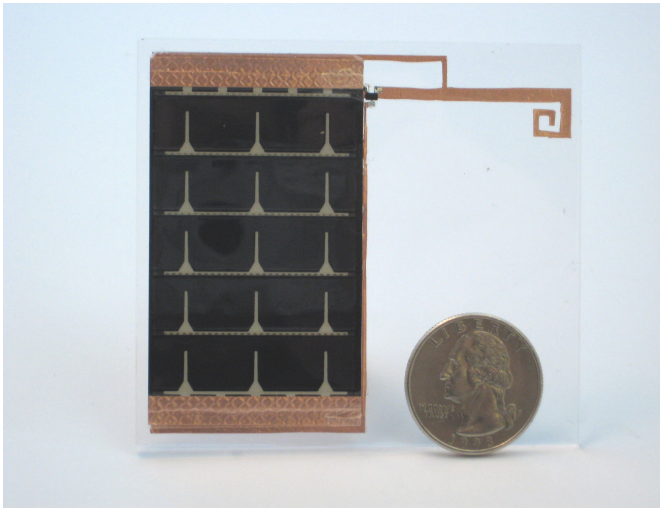

Figure 3. Image of the photovoltaic-enhanced RFID antenna connected to an Alien Higgs-3 SOT-323 packaged RFID IC. The solar cell is manufactured by Powerfilm Inc. part number #SP3-37. The completed tag prototype has been mounted to a 1mm thick layer of Plexiglas for rigidity. This tag shows the viability of incorporating photovoltaics into RFID antennas while maintaining RF performance. (For clarity, this IC does not accept solar power).

The Powerfilm solar cell was modified to expose the bus bars from the underside. It was then gently soldered to the copper traces of the antenna. Lastly, an Alien Higgs-3 SOT-323 packaged RFID IC was soldered to the antenna to complete the RFID tag. Again, the Higgs-3 tag is not able to use the DC power provided by the solar cell because the appropriate net is not exposed. However, the completed device does represent a tag-compatible antenna design which can be used to verify the RF performance of the photovoltaic-enhanced antenna.

Simulation results show that the antenna has a maximum gain of 1.7 dBi and a radiation pattern typical of a dipole antenna. Considering the complexity of the solar panel's construction and material characteristics, simulations were run using a simple all-copper model with identical dimensions. Because the simulation was simplified in this manner, it is important to show that the addition of the photovoltaic material does not significantly alter the RF performance of the antenna. Figure 4 shows plots of the simulated input impedance, the measured input impedance of a copper-only version, and the measured input impedance of the full photovoltaic-enhanced antenna as shown in Figure 3. The impedance plots show that the solar antenna's reactance is slightly lower than that of the all-copper version, a difference small enough to be easily compensated for in future design cycles. Essentially, these results indicate that the solar panel is acting as a conductor at UHF frequencies.

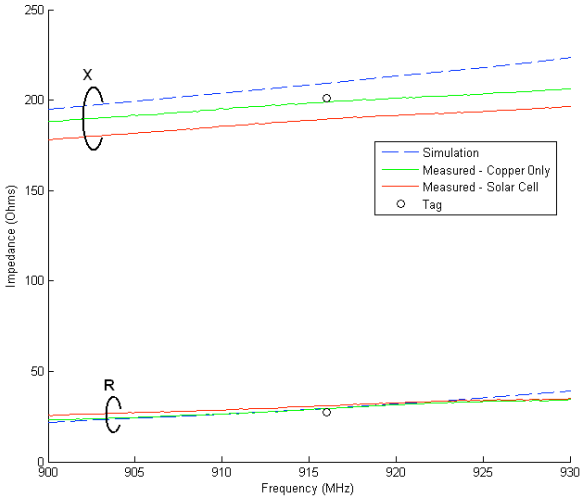

Figure 4. Simulated and measured input impedances for the IC specific solar antenna. The bottom group of traces shows the real impedance and the top group shows the complex. Measurements show a small deviation between the copper version of the antenna and the antenna the cooperates the solar cell.

Next, the read range of the photovoltaic-enhanced antenna plus Higgs-3 IC was tested for read range. In order to reduce the effects of multipath interference, a variable RF attenuator was used to simulate changes in distance. The reader antenna and tag were placed 0.75 meters apart and both were placed one meter above the ground. Care was taken to minimize reflections in the immediate environment. Figure 5 shows a plot of the equivalent distance, calculated using the Friis equation, which was determined to be comparable to commercial tags. Measurements show that tag sensitivity is approximately 1 dB lower than predicted using the simulated antenna gain and the IC manufacturer's specified RF sensitivity. This is attributed to the small impedance mismatch seen in Figure 4 and manufacturing variation of the antenna geometry.

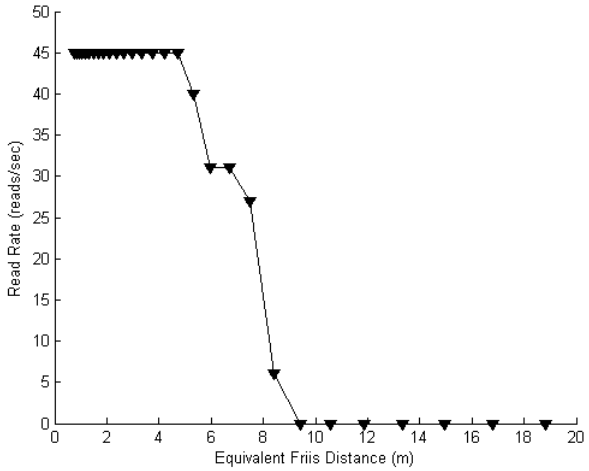

Figure 5. Read range of the prototype photovoltaic-enhanced RFID tag, using the Higgs-3 IC. Solar power was not used by the IC.

B. Solar WISP Antenna Design

In order to explore the performance gains of a complete photovoltaic-enhanced RFID tag that can use the harvested solar power, a second antenna, intended for use with the WISP 4.1, has been prototyped. The antenna design, shown in Figure 6, is a modified inverted F and connects to the WISP through vias in the antenna's substrate. This antenna, with attached WISP, is shown in Figure 7.

A thin trace connects the positive bus of the solar cell to the unregulated power supply of the WISP to transfer the harvested solar power to the WISP. The DC trace is thin so that it appears as a high-impedance port to the RF signal on the antenna and thus filters out the RF signal from the DC port. In the prototype design, a Schottky diode is added to the WISP to ensure that, when the solar cell has a lower voltage than the unregulated power supply on the WISP, the WISP will not shunt harvested RF power into the solar cell.

The input impedance of this antenna is 40 + j150 and can be easily matched to the WISP's rectifier using the discrete L-match network that is integrated to the WISP's analog-front-end. One common misconception is that the WISP requires a balun to convert the balanced antenna signal to the unbalanced analog-front-end. As is the case with most RFID tags, this step is not necessary and would cause undue loss of precious RF signal. The reasoning for the lack of a balun is that RFID tags have very low capacitive coupling to earth ground, thus their GND plane (or silicon substrate) can truly float with respect to earth ground. The same argument is true for the WISP. The only caveat is that the GND plane on the WISP is oscillating at 915MHz, and therefore care must be taken when connecting probes and long wires.

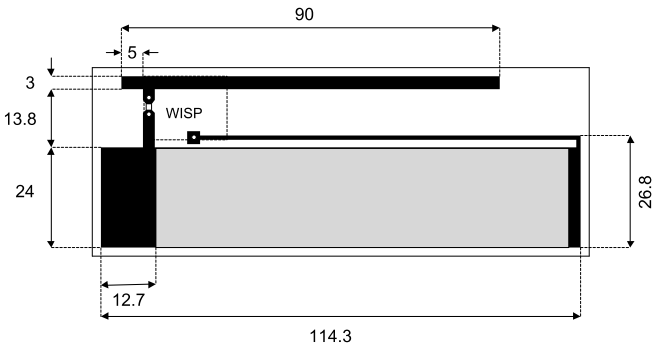

Figure 6. Solar-enhanced antenna design for WISP-based tag.

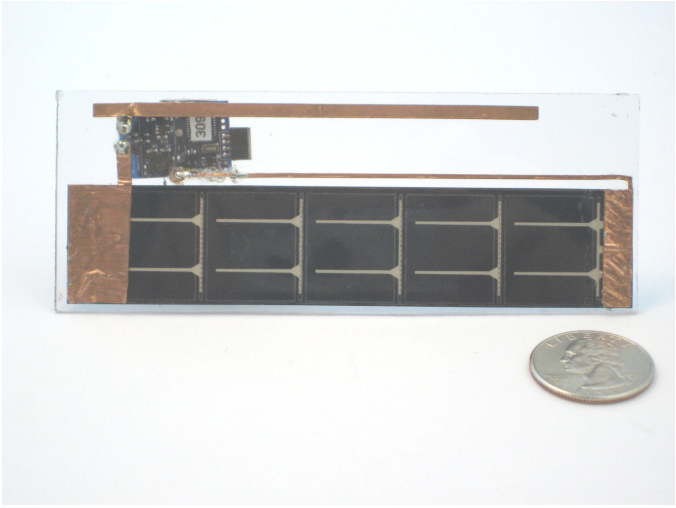

Figure 7. Folded Dipole With Solar Cell. (a) Front. (b) Back.

C. *Range improvement for Solar WISP*

After characterizing the impact of replacing a standard copper antenna with a solar panel, the next step is to quantify the performance increase and additional benefits that the solar-enhanced antenna enables. Expected benefits of solar augmentation are an increase in read rate and range, as well as the ability to perform functions such as computation and data logging while away from the reader.

Increasing the read range of RFID systems is an ongoing effort within the RFID community, as increased range allows for increased usability and a greater variety of applications. For instance, RFID sensor networks, which are composed of many tags with onboard sensing capabilities, could be made communicate faster and operate over larger areas using solar-enhanced tags rather than purely RF-powered devices. The following experiment characterizes the read range improvements provided by the solar-enhanced antenna.

As described in Section III.B., a solar antenna was conjugate matched to the RF front end of a WISP using an onboard discrete matching network. To quantify the range benefits of the solar antenna, the read rate of the attached WISP was measured as a function of simulated reader-to-tag distance under various lighting conditions and in the absence of light. In order to determine an upper limit for read range when available power is not a constraint, the solar antenna-based WISP was then externally powered using a battery and its performance measured.

The device was placed 0.75m away from an RFID reader in a room that was made to have as little multipath interference as possible. A variable RF attenuator was inserted between the reader antenna and an Impinj Speedway reader to serve as free-space loss for various tag distances. This attenuator was used instead of physically moving the tag in order to eliminate the effect of changes in multipath interference patterns which would occur if the tag were moved. An incandescent light source was used to provide known lighting conditions for the solar-enhanced WISP, as measured by a Sper Scientific® 840022 light meter. Lighting conditions for the solar-enhanced tag represent a variety of environments in which the tag might be used, and were each chosen to be near to minimum lighting requirements for those environments specified by the Occupational Safety and Health Administration [16].

The read rate of the solar-enhanced WISP was measured under four different lighting conditions at each of 31 attenuation levels, which simulate reader-to-tag distance. Figure 8 shows the resulting read rate vs. distance plot.

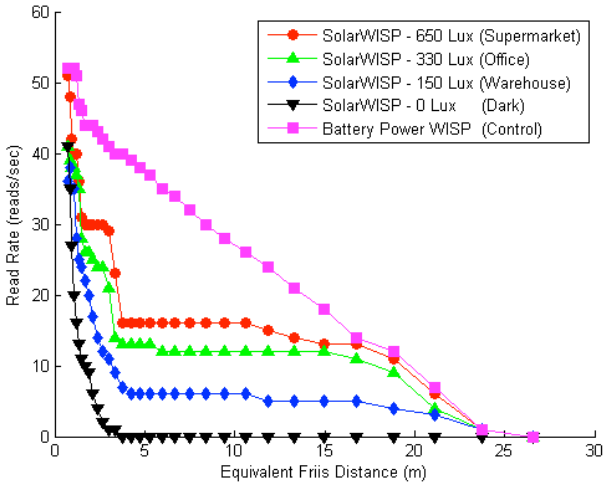

Figure 8. Read rate as a function of distance for WISP tags using the solar-enhanced antenna tag and solar antenna tag with externally-supplied DC power. Equivalent distance is calculated assuming a 1 Watt transmitter.

Using a 1-Watt transmitter, the solar antenna-based WISP with 150 lux of incident light was readable from up to 24 m. In contrast, the darkened solar antenna with less than 1 lux of incident light had a read range of only 4 m. However, as incident light intensity was increased from 150 lux to 330 and then to 650, maximum read range did not significantly increase. Additionally, the battery-powered tag had a similar maximum read range to the solar powered devices. This near equivalence in range between each of the solar-powered tags and the externally supplied tag suggests that the determined maximum range in this experiment was limited by reader or tag sensitivity, rather than by available power. A more sensitive reader could likely be used to further enhance the read range of these solar-augmented tags.

An interesting feature of the solar-augmented read rate plot is the sudden decrease in read rate as the simulated distance passes 4 m. This drop occurs at the point when the RF power provided by the reader is no longer sufficient to bias the harvesting circuit. At distances greater than 4 m the tags are entirely powered by the lit solar antenna, and so read rate becomes relatively constant with respect to reader-to-tag distance. Increasing the available power by increasing light intensity or adding an external supply significantly increases read rates for the solar-enhanced WISP, particularly at distances over 4 m where RF power is not a factor.

IV. Reader Independent Operations

As well as increasing the RFID read range of a tag, the addition of a solar antenna allows the tag to become operational even when out of range of an RFID reader. This enables a solar antenna-based tag to perform sensing, data logging, computation, and other functions in any scenario where sufficient light is available. There are several foreseeable applications where it is desirable for a tag to perform sensing and data logging away from the reader. For instance, cold chain monitoring of food and pharmaceuticals could be improved through the use of data logging solar-enhanced tags, which could verify that products remained within a given temperature range throughout their processing and shipment. Sensitive equipment traveling across the country could also be augmented with temperature and orientation-logging tags which would enable shipping companies or the recipients of the shipment to determine what conditions the equipment had been exposed to during its journey. This experiment will explore the latter application by using a solar antenna-based WISP tag, shown in Figure 9, to log a parcel's temperature and orientation throughout a simulated shipment.

Figure 9. Passive solar antenna-based data logger on a parcel.

RFID tags have already found widespread application in shipping and parcel tracking. Use of a solar antenna-based enhanced-RFID tag could allow for important parameters of a parcel's condition to be recorded throughout its entire route without the need for an RFID reader to accompany the tagged item and provide power to the tag. Arranging for RFID readers to be present in each stage of a shipment would be prohibitively expensive due to the cost of the reader, associated hardware, and infrastructure required. A cost-effective alternative which would allow for continuous data logging could be implemented with the simple addition of a light source to the inside of the shipping container or delivery vehicle, which would provide power for solar antenna-based data logging tags.

The solar antenna-based WISP is programmed such that, when ambient light conditions provide sufficient power, the device will take measurements from an onboard temperature sensor and 3-axis accelerometer and record these measurements to an EEPROM. The state diagram in Figure 10 provides an overview of the firmware design for the data-logging WISP. While out of range of the RFID reader, the device firmware puts the WISP into a low-power mode. In this state, the solar antenna charges a storage capacitor which provides power for the WISP's microcontroller and various subsystems. Each second, a watch crystal-based timing circuit wakes the device, and data logging operations are performed. A 32.768 kHz watch crystal was chosen as the time base because it provides a high degree of accuracy with minimal power cost.

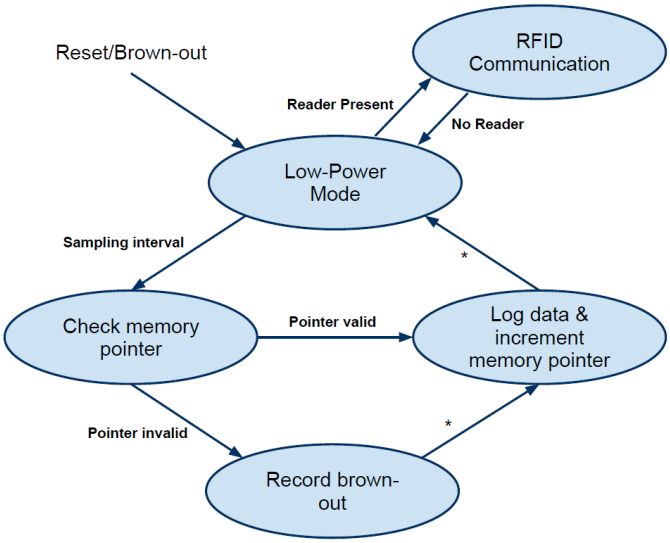

Figure 10. State diagram for solar-enhanced, data-logging WISP.

In the case where there is insufficient ambient light to support the timing circuit's operation, the device will "brown out," or lose power, and log the event. Any such loss of power recorded in the data log indicates that the tag has lost track of time, rendering timing information for the remainder of the data log inaccurate. This detection of brown-out events is accomplished by comparing a pointer value in the microcontroller's volatile memory to a value in the non-volatile EEPROM. In normal operation, the two values should always be equal. If the two pointer values differ, it can be assumed that a brown-out reset event has occurred.

When the device re-enters a reader's field and is queried by the reader, temperature and acceleration measurements recorded to the onboard EEPROM are sequentially transmitted to the reader. For simplicity, the data is transmitted as part of the tag's EPC, although in a real-world application the data would likely be sent in response to a read command.

In the simulated shipment, a parcel with the RFID data logger attached is carried around an office floor under typical lighting conditions, starting and ending within range of an RFID reader. Data is collected during the period when the tag is outside the reader's range. The plot in Figure 11 contains the temperature, 3-axis acceleration, and brown-out events recorded by the tag. The tag is exposed to sufficient light for most of its trip, only experiencing a loss of power once at 215 seconds into the trip when it is placed in a darkened area. Several times during its travel, the parcel is placed on its side and the accelerometer detects an orientation change. To demonstrate temperature sensitivity, the parcel is heated under a lamp from the 50 to 100 second mark, and allowed to cool for the remainder of its trip.

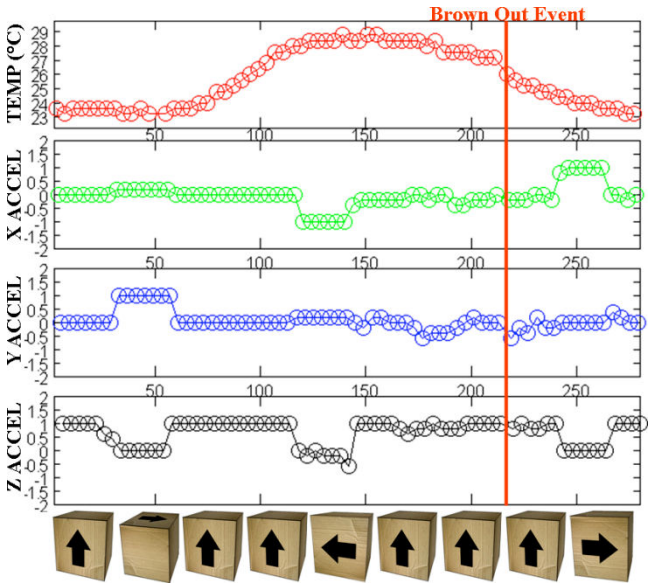

Figure 11. Temperature and orientation data recorded by the solar-enhanced RFID platform during a simulated parcel shipment.

Applications for such a solar antenna data logging device are constrained by power limitations. The light intensity necessary to perform data-logging operations will depend on such factors as the size and conversion efficiency of the solar antenna, the desired sampling interval, and the power requirements of the sensors and non-volatile memory used. Sensors and memory devices for this experimental setup were chosen for their low power requirements. An ultra low-power Texas Instruments® MSP430 microcontroller implements the computation and control functions for the system, as well as the EPC Gen 2 RFID protocol. A 1 kB Microchip® EEPROM provides non-volatile storage of logged data. Acceleration data is produced by an Analog Devices® ADXL330 MEMS accelerometer.

Uses that require a high sensor sampling rate, or that require sensors to be continuously powered, will not likely be possible in such a system. For example, it would be difficult to use this device to measure the maximum acceleration experienced by a parcel, as this requires very fast sampling or continuous sensor operation. However, as sensing technologies advance and power requirements decrease, more and more applications will become possible with this system.

Aside from power considerations, another concern which must be addressed before this system can be fully implemented is the amount of time required for the data logging RFID device to transmit its recorded history to the reader upon arrival at its destination. Procedures at the receiving station may need to be modified to allow the parcel-attached tag sufficient time to transmit all of its memory contents. To mitigate this issue, the tag could analyze the data during recording and identify important events, which it would then transmit first when within range of the reader. Power provided by the solar antenna allows for computation and data interpretation tasks such as this to take place on the tag itself, prior to encountering the reader.

V. Conclusions

This paper has argued that the most challenging obstacle to improving passive RFID tag performance is the limited amount of power that can be rectified from the signal transmitted by the RFID reader. In order to augment this power supply, a novel, dual purpose RFID tag antenna that simultaneously harvests RF energy, communicates with the RFID reader, and harvests solar energy has been proposed.

A prototype of the solar-enhanced RFID antenna has been built and simulated in HFSS. Intel Lab's WISP (an RFID development platform) was used to create and test a complete working prototype of a solar antenna-based RFID tag. The dual-harvesting antenna increased the effective read range of the tag by at least a factor of six under typical indoor office illumination conditions. In the same indoor lighting conditions, enough power was available to perform sensing and data logging, even while away from an RFID reader. The dual harvesting strategy presented here can enhance the read rate of RFID tags, provide increased power for more demanding workloads such as sensing and computation, and allow sensing, data logging, and computing operations away from RFID readers.

The tag architecture is compatible with low cost, high volume production processes. Since most existing UHF RFID tag ICs have 4 contacts (including two redundant ground pads), the hybrid solar-RF antennas presented here are compatible with existing RFID IC footprints. Photovoltaic harvesting materials can be printed using low-cost, high volume processes compatible with RFID manufacture, and thus it should be possible to integrate the photovoltaic and RFID manufacturing processes without extensive modification. The end result will be tags that are similar in cost to today's ordinary RFID tags, but with improved performance and additional capabilities enabled by the additional power source.

REFERENCES

[1] Namjun, Cho, et al, "A 5.1-µW 0.3-mm2 UHF RFID Tag Chip Integrated With Sensors for Wireless Environmental Monitoring," *IEEE European Solid State Circuits Conference*, September, 2005, Grenoble, France. Pp. 279- 282.

[2] Kocer, F. and M. P. Flynn. "A new transponder architecture with on-chip ADC for long-range telemetry applications," *IEEE Journal of Solid-State Circuits*, vol. 41, no. 5, May 2006, pp. 1142-1148.

[3] Hee-Jin Chae, Daniel J. Yeager, Joshua R. Smith, Kevin Fu. "Maximalist Cryptography and Computation on the WISP UHF RFID Tag," *Conference on RFID Security*, July 2007

[4] Sample, A.P.; Yeager, D.J.; Powledge, P.S.; Mamishev, A.V.; Smith, J.R., "Design of an RFID-Based Battery-Free Programmable Sensing Platform," *IEEE Transactions on Instrumentation and Measurement*, vol.57, no.11, pp.2608-2615, Nov. 2008

[5] Yeager, D.J.; Powledge, P.S.; Prasad, R.; Wetherall, D.; Smith, J.R., "Wirelessly-Charged UHF Tags for Sensor Data Collection," *IEEE International Conference on RFID, 2008*, vol., no., pp.320-327, 16-17 April 2008

[6] Sample, A.P.; Yeager, D.J.; Smith, J.R., "A capacitive touch interface for passive RFID tags," *IEEE International Conference on RFID*, pp.103-109, 27-28 April 2009

[7] Paradiso, J.A.; Starner, T., "Energy scavenging for mobile and wireless electronics," *Pervasive Computing, IEEE*, vol.4, no.1, pp. 18-27, Jan.-March 2005

[8] Clark, S; Gummeson, J; Fu, K; and Ganesan. D;. "Towards Autonomously-Powered CRFIDs," *Workshop on Power Aware Computing and Systems*, October 2009.

[9] Vyas, R.; Lakafosis, V.; Konstas, Z.; Tentzeris, M.M., "Design and characterization of a novel battery-less, solar powered wireless tag for enhanced-range remote tracking applications," *Microwave Conference, 2009. EuMC 2009. European*, vol., no., pp.169-172, Sept. 29 2009-Oct. 1 2009

[10] Raghu, Das, and Peter Harrop. Organic and Printed Electronics in North America (2009): 351. Web. 7 Dec 2009. <http://www.idtechex.com/research/reports/organic_and_printed_electronics_in_north_america_000188.asp>.

[11] Henze, N.; Weitz, M.; Hofmann, P.; Bendel, C.; Kirchhof, J.; Fruchting, H., "Investigation of planar antennas with photovoltaic solar cells for mobile communications," *Personal, Indoor and Mobile Radio Communications*, 2004. PIMRC 2004. 15th IEEE International Symposium on , vol.1, no., pp. 622-626 Vol.1, 5-8 Sept. 2004

[12] Vaccaro, S.; Mosig, J.R.; de Maagt, P., "Two advanced solar antenna "SOLANT" designs for satellite and terrestrial communications," *IEEE Transactions on Antennas and Propagation*, vol.51, no.8, pp. 2028-2034, Aug. 2003

[13] Shynu, S.V.; Roo Ons, M.J.; Ammann, M.J.; McCormack, S.; Norton, B., "Dual band a-Si:H solar-slot antenna for 2.4/5.2GHz WLAN applications," *Antennas and Propagation*, 2009. EuCAP 2009. 3rd European Conference on , vol., no., pp.408-410, 23-27 March 2009

[14] Kiefer, Karl F. "Combination Photovoltaic Cell and RF Antenna and Method." U.S. Patent 6 590 150, Jul. 8, 2003.

[15] Marrocco, G., "The art of UHF RFID antenna design: impedance-matching and size-reduction techniques," *Antennas and Propagation Magazine, IEEE*, vol.50, no.1, pp.66-79, Feb. 2008

[16] United States Department of Labor; Minimum Illumination Intensities in Foot-Candles http://www.osha.gov/pls/oshaweb/owadisp.show_document?p_table=standards&p_id=10630

[17] WISP WIKI Website http://wisp.wikispaces.com/WISPMonitor

[18] Paul Schlyter; Radiometry and Photometry in Astronomy http://stjarnhimlen.se/comp/radfaq.html#10